Astron. Astrophys. 344, 143–150 (1999)

ASTRONOMY AND ASTROPHYSICS

The orientation within the Galaxy and the Large Magellanic Cloud of nebulae ejected by massive stars⋆

D. Hutsemékers⋆⋆

Institut d'Astrophysique, Université de Liège, 5 av. de Cointe, B-4000 Liège, Belgium

Received 27 April 1998 / Accepted 5 January 1999

Abstract. The orientation of nebulae ejected by massive stars (Luminous Blue Variables, WR stars, SN1987A) is investigated with respect to the structure of the galaxy to which they belong.

In the Galaxy, we find that the projected long axes of the nebulae most often align with the galactic plane, and then also with the galactic magnetic field. This alignment is statistically significant. In addition, a few nebulae are apparently oriented perpendicular to the galactic plane. In the Large Magellanic Cloud, the nebular axes are found to closely follow the spiral magnetic field. With different inclinations, the Galaxy and the Large Magellanic Cloud probably offer complementary views of the same phenomenon.

Although the sample studied thus far is small and the statistics limited, these results suggest that the orientation of massive star ejecta depends on galactic magnetic fields.

Since the nebular axes are apparently correlated to the symmetry axes of the stars themselves, and since, in the early evolutionary stages, alignments of accretion disk axes with the interstellar magnetic field have been reported, it is argued that the observed alignment effect results from the star formation process.

Key words: stars: circumstellar matter – stars: early-type – stars: supernovae: individual: SN 1987A – stars: Wolf-Rayet – ISM: magnetic fields – galaxies: Magellanic Clouds

1. Introduction

The orientation of stars, their outflows or their associated nebulae with respect to their environment, either local or global, may provide insights on their formation, life, and death in interrelation with the surrounding medium, i.e. their ecology.

Flows and jets from young objects are known to frequently align with the ambient interstellar magnetic field, a result of great importance for the theoretical interpretation of the flows as well as for star formation theory (e.g. Strom et al. 1988, Appenzeller 1989, and references therein).

At the other end of stellar evolution, the orientation of planetary nebulae with respect to the galactic plane has been studied by Grinin & Zvereva (1968), Melnick & Harwit (1975), and Phillips (1997). Considering a large sample of objects, all these authors found a significant alignment of planetary nebula major axes with the galactic plane, an effect which indicates a possible influence of the galactic magnetic field. Apparently, no clear theoretical modelling accounts for this phenomenon (cf. Phillips 1997).

Like planetary nebulae, which are ejected by evolved low-mass stars, nebulae are also ejected by the most massive stars in the late stages of their evolution. Such nebulae are detected around Luminous Blue Variables (LBV) and Wolf-Rayet (WR) stars. An alignment between the long axis of the nebulae surrounding the LBVs R127, AG Car and η Car and the direction of the local interstellar polarization –an indicator of the magnetic field local direction– has already been noticed by Schulte-Ladbeck et al. (1993, 1994) and Aitken et al. (1995). In fact, the position angles of the η Car, AG Car and HR Car nebulae (as reported in the literature, cf. Appendix A) are remarkably similar, possibly indicating a more global alignment effect.

The aim of the present paper is to study on a statistical basis the orientation of all known galactic LBV nebulae (plus a few ring nebulae associated with WR stars) with respect to the galactic plane and to the local direction of the interstellar polarization. LBV nebulae resolved in the Large Magellanic Cloud (LMC) are also considered and their orientation compared to the direction of the LMC magnetic field. In Sect. 2, the definition of the sample and the measurements of nebular position angles are described. Statistical analyzes and results are presented in Sect. 3, while discussion and conclusions form the last section.

2. The sample and the measurements

The sample contains all known nebulae associated with galactic LBVs and LBV candidates (Nota & Clampin 1997, Hutsemékers 1994, 1997). All these nebulae are recognized to be dusty stellar ejecta. Only two LBVs, HD168607 and HD160529, are not surrounded by nebulae although imaged in similar conditions. To this sample we add the four WR ring nebulae known

⋆ Based in part on observations collected at the European Southern Observatory (ESO, La Silla)

⋆⋆ Also, Chercheur Qualifié au Fonds National de la Recherche Scientifique (FNRS Belgium)

Correspondence to: hutsemek@astro.ulg.ac.be

to be mainly constituted of matter ejected by the star: M1-67, RCW58, NGC6888, and S308 (Smith 1995). Other WR ring nebulae are essentially constituted of interstellar gas and are not considered here. The only LBV nebula for which no preferential axis can be defined is that around P Cygni. Interestingly, it has also several peculiarities which distinguish it from other LBV nebulae (Nota et al. 1995, Hutsemékers 1997). Finally, the total sample amounts to twelve galactic nebulae. All objects are at low galactic latitudes.

While there are as many LBVs in the LMC as in the Galaxy, the consequence of the larger distance to the LMC is that only two nebulae (those around R127 and S119) are resolved with enough detail to reveal their morphology and the association with the central star (e.g. Nota & Clampin 1997). Among WR ring nebula resolved in the LMC, only that one surrounding Br13 is presently confirmed as an ejecta (Garnett & Chu 1994). In addition, we also consider the famous three-ring nebula associated with SN1987A (Burrows et al. 1995). Although its exact nature is still unclear and not strictly related to LBV or WR ring nebulae, it is nevertheless constituted of material ejected by the massive supernova progenitor (Panagia et al. 1996). Excited by the supernova ultraviolet flash, this nebula may therefore represent an advanced, short-lived, stage of nebulae ejected by massive stars.

The adopted nebular position angles refer to the projected morphological long axes of the nebulae whatever their type, i.e. true bipolar or elliptical. As suggested by Nota et al. (1995), both morphologies may result from a unique shaping mechanism as in the case of planetary nebulae. Bipolar nebulae (e.g. HD168625) often have a "waist" i.e. a brighter ring[1] perpendicular to the long (bipolar) axis. For elliptical nebulae, this waist manifests itself as emission enhancement along the minor axis (e.g. AG Car). However, there may be some ambiguity about the exact morphological type. Indeed, some elliptical nebulae could in fact be bipolar objects seen along the bipolar axis, or even the brighter waists of bipolar nebulae with very faint and undetected lobes. In the latter case the measured position angle will be perpendicular to the true long axis, while in the former one, morphological details will affect the measurements. Ideally, one should have used only fully developed bipolar nebulae to detect at best a possible alignment effect. But, in our case, this reduces the sample too drastically for it to remain statistically useful. We therefore consider all the nebulae of the sample at the risk of masking a possible deviation from a random orientation of axes.

The nebular morphological long axes are determined from narrow-band visible images (mostly Hα). For the two highly reddened objects G25.5+0.2 and G79.29+0.46, optical images are not available and radio maps are used. In addition to values explicitly provided in the literature, the nebular position angles are measured on published images, as well as on several Hα+[N II] images that we obtained ourselves with the ESO 3.6m telescope equipped with EFOSC1 in its coronographic mode (cf. Hutsemékers et al. 1994 for technical information). The measurements for individual objects are detailed in Appendix A. The uncertainties of position angles are estimated from the dispersion of measurements obtained after several trials and combined with measurements given in the literature if any. They are typically around 5°. It should be noted that even in situations where the ellipticity of the nebula is small, or when the overall nebular morphology is dubious, one may define a preferential axis with a reasonable accuracy. This is the case of the nebulae S308 and G79.29+0.46 which are nearly circular, and for WRA751 and M1-67 which cannot be unambiguously classified as bipolar or elliptical, but which are clearly elongated. Possible errors due to a mis-interpretation of the observed nebular morphological features can however not be excluded. It is therefore important to emphasize that possible errors on position angles or morphological types, systematic or not, can only act to reduce the deviation from a uniform distribution and certainly not to produce coherent orientations. Also, possible biases in the data (lack of independence) are minimized. Indeed, the position angles are measured in the equatorial coordinate system before being transformed into position angles in the galactic coordinate system in which the alignments are finally searched for.

The resulting position angles are given in Tables 1 and 2, together with the object distance d, the galactic longitude $l_{\rm II}$ and galactic latitude $b_{\rm II}$, or the right ascension α and declination δ.

Table 1. The sample of galactic nebulae

Object	d (kpc)	$l_{\rm II}$ (°)	$b_{\rm II}$ (°)	$\theta_{\rm E}$ (°)	σ_θ (°)	$\theta_{\rm G}$ (°)	$\Delta_{\rm G}$ (°)
HD168625	2.2	15.0	−1.0	29	5	90	0
G25.5+0.2	14.0	25.5	+0.2	128	5	10	80
M1-67	4.5	50.2	+3.3	25	10	87	3
NGC6888	1.8	75.5	+2.4	38	3	94	4
G79.29+0.46	2.0	79.3	+0.5	45	10	98	8
S308	1.8	234.8	−10.1	146	10	81	9
HR Car	5.2	285.1	−2.0	130	5	97	7
η Car	2.5	287.6	−0.6	132	2	104	14
He3-519	7.6	288.9	−0.8	34	5	8	82
AG Car	6.0	289.2	−0.7	132	3	106	16
WRA751	7.1	290.7	−0.3	155	10	132	42
RCW58	2.5	292.3	−4.8	8	5	164	74

Table 2. The sample of LMC nebulae

Object	α (°)	δ (°)	$\theta_{\rm E}$ (°)	σ_θ (°)	$\Delta_{\rm B}$ (°)
Br13	75.8	−66.8	47	3	1
S119	83.0	−69.1	133	5	8
SN1987A	84.0	−69.3	168	5	15
R127	84.3	−69.5	180	10	25

[1] We emphasize that only the projected morphology is considered here, independently of the kinematics and the actual three-dimensional morphology. For example, the elliptical nebula around AG Car is essentially an expanding shell (Smith 1991), while the observed ring around HD168625 is in fact an expanding shell on which a bipolar outflow is apparently superimposed (Hutsemékers et al. 1994). Note that in most cases, the three-dimensional morphology is still unclear or controversial

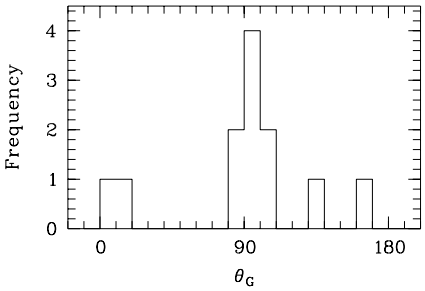

Fig. 1. The distribution of $\theta_{\rm G}$, the position angle of the long axes of galactic LBV and WR nebulae

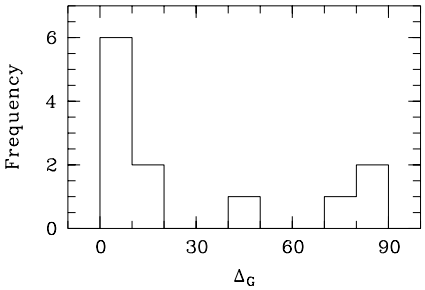

Fig. 2. The distribution of $\Delta_{\rm G}$, the position angle relative to the plane of the Galaxy of the long axes of galactic LBV and WR nebulae

$\theta_{\rm E}$ and $\theta_{\rm G}$ respectively refer to the position angles expressed in the equatorial and galactic coordinate systems. In agreement with the usual convention, the equatorial position angle $\theta_{\rm E}$ (= P.A. in Appendix A) refers to the direction of the nebular axis projected onto the plane of the sky, and measured from the north ($\theta_{\rm E} = 0°$) towards the east ($\theta_{\rm E} = 90°$). The galactic position angle $\theta_{\rm G}$ similarly refers to the direction of the projected nebular axis but now measured from the galactic north ($\theta_{\rm G} = 0°$) towards the galactic east ($\theta_{\rm G} = 90°$). Both position angles are defined from $0°$ to $180°$. They are related by

$$\tan(\theta_{\rm G} - \theta_{\rm E}) = \frac{\cos b_p \, \sin(l_p - l_{\rm II})}{\sin b_p \, \cos b_{\rm II} - \sin b_{\rm II} \, \cos b_p \, \cos(l_p - l_{\rm II})} \quad (1)$$

where $l_p = 123\overset{\circ}{.}0$ and $b_p = 27\overset{\circ}{.}4$ are the galactic coordinates of the equatorial north pole. σ_θ represents the uncertainty of the position angle estimated in Appendix A. For the galactic objects, $\Delta_{\rm G} = |\theta_{\rm G} - 90°|$ is the acute angle between the nebular long axis projected onto the plane of the sky and the galactic plane (all objects roughly lie in the galactic plane). For LMC objects, $\Delta_{\rm B}$ represents the difference between the nebular position angle and a local average of the magnetic field direction (see Sect. 3.3).

3. The alignment effect

3.1. Alignment of galactic nebulae with the galactic plane

Fig. 1 illustrates the distribution of the nebular position angles $\theta_{\rm G}$. It is immediately clear that the distribution is apparently not uniform and has a strong peak near $\theta_{\rm G} \simeq 90°$, indicating an alignment with the galactic plane. Considering the two bins centred on $90°$, the expected mean is 12/9 and the observed excess a 4σ deviation. Another smaller peak is seen around $\theta_{\rm G} \simeq 0° \ (\simeq 180°)$ indicating that some objects are oriented perpendicular to the galactic plane[2]. These tendencies are more clearly seen in Fig. 2 which illustrates the distribution of $\Delta_{\rm G}$, the position angle relative to the plane of the Galaxy. The median of $\Delta_{\rm G}$, noted $\tilde{\Delta}_{\rm G}$, is equal to $11\overset{\circ}{.}5$; it is significantly different from $45°$, the value expected from a uniform distribution.

For evaluating the significance of a possible alignment effect, it is important to recall that the observed position angle $\theta_{\rm G}$ refers to the object long axis projected onto the plane of the sky. If nebular axes are randomly oriented in the three dimensional (3D) space (which is equivalent to uniformly distributing points on the surface of a sphere), all axes characterized by a given $\theta_{\rm G}$ are located on a great circle, such that the projected position angles $\theta_{\rm G}$ are equally likely[3]. Hence, randomly oriented nebular axes have uniform distributions in $\theta_{\rm G}$ and $\Delta_{\rm G}$.

Statistical tests may then be used to see if the position angles are drawn from a uniform distribution, or not. Note that statistics for circular data (e.g. Fisher 1993) are needed when analyzing the angles $\theta_{\rm G}$, while usual linear statistics are adequate for $\Delta_{\rm G}$. We therefore apply the well-known Kolmogorov-Smirnov (K-S) test to the distribution of $\Delta_{\rm G}$. The K-S statistic is computed to be $D = 0.489$ for $n = 12$ objects. This corresponds to a probability $P_{\rm K-S} = 6\,10^{-3}$ that the observed distribution of $\Delta_{\rm G}$ is drawn from a uniform distribution. This suggests a significant deviation from uniformity.

However, such a test does not identify the nature of the deviation, and does not provide an estimate of the significance of the possible alignment. A rather simple measure of the angle concentration near $\Delta_{\rm G} \simeq 0°$ is the median of the distribution. We therefore adopt this quantity as a statistic and evaluate the probability to obtain by chance only a value of the median $\tilde{\Delta}_{\rm G} \leq 11\overset{\circ}{.}5$, assuming the angles $\Delta_{\rm G}$ uniformly distributed. For this, we randomly generate 10^5 sets of 12 angles $\Delta_{\rm G}$. The median is computed for each set, and its distribution built from the 10^5 realizations. From this distribution, we derive a probability $P_{\rm M} = 4\,10^{-4}$ that the observed value of the median is due to chance only, which indicates a significant alignment effect.

In order to see if this result is stable against uncertainties, we now randomly choose for each object its position angle in the interval $[\theta_{\rm G} - \sigma_\theta, \theta_{\rm G} + \sigma_\theta]$ assuming uniform deviates. For the 12 objects of the sample, a new median $\tilde{\Delta}_{\rm G}$ is then computed. By

[2] Note a possible –small– systematic difference of 5–10° with the maxima at 90° and 180°. This is also apparent in Fig. 4

[3] This is definitely not the case for the orientation angle θ, defined as the angle between the object true long axis and the polar ($b_{\rm II}$) axis, such that $\Delta = |90° - \theta|$ represents the true (3D) orientation of the nebula with respect to the galactic plane. Indeed, when the axes are randomly oriented in the 3D space, these angles are not uniformly distributed: they are biased towards alignment with the galactic plane. Assuming the objects located in the galactic plane, this may be seen from the relation $\tan\theta = \tan\theta_{\rm G} \,/\, \sin\phi_{\rm G}$, where $\phi_{\rm G}$ is the angle between the line of sight (r axis) and the object long axis projected onto the galactic plane (i.e. the (r, $l_{\rm II}$) plane). Like $\theta_{\rm G}$, the angle $\phi_{\rm G}$ is uniformly distributed for random orientations of axes in the 3D space (see also Fisher et al. 1987)

repeating this process 10^4 times, we derive the distribution of $\tilde{\Delta}_{\rm G}$, which appears to be roughly normal with a mean $<\tilde{\Delta}_{\rm G}>$ = $13\overset{\circ}{.}1$ and a standard deviation $1\overset{\circ}{.}7$. The median of the observed sample therefore lies within the 3σ confidence interval [$8\overset{\circ}{.}0$, $18\overset{\circ}{.}2$] and probability that it is due to chance only is computed to be between $P_{\rm M} = 6\,10^{-5}$ and $P_{\rm M} = 7\,10^{-3}$. These values still indicates a significant deviation from uniformity.

Finally, if we simply discard from the sample the four nebulae with more uncertain measurements, i.e. M1-67, G79.29+0.46, S308 and WRA751 (cf. Sect. 2), the median is computed to be $\tilde{\Delta}_{\rm G}$ = 15.0 for n = 8 objects, a value which has a probability $P_{\rm M} = 8\,10^{-3}$ to be due to chance only.

We may therefore safely conclude that the major axes of the nebulae around LBV and WR stars are not randomly oriented, and that a significant tendency to alignment with the galactic plane is detected, even within our rather small sample.

Given this overall alignment, it is interesting to note that all but one misaligned nebulae have their axis nearly perpendicular to the galactic plane (Fig. 2). Although this weak tendency could be real, one should remark that two of these objects, He3-519 and RCW58, are both elliptical nebulae older and fainter than e.g. the AG Car nebula and therefore possibly affected by errors on their true morphological type (cf. Sect. 2), while the classification as a LBV-type nebula of the third object, G25.5+0.2, is still hypothetical (Subrahmanyan et al. 1993, Hutsemékers 1997).

3.2. Alignment of nebulae with the interstellar polarization in the Galaxy

Many distant stars are polarized in the visible due to dichroic absorption by aligned interstellar dust grains. The direction of this interstellar polarization is thought to follow the direction of the galactic magnetic field (e.g. Mathewson & Ford 1970, Axon & Ellis 1976). Since at the low latitudes where our objects lie, the magnetic field is essentially parallel to the galactic plane, the correlation found in the previous section will necessarily repeat itself when comparing the nebular position angles to the polarization position angles of neighbouring objects. However, there is some variation in the orientation of the interstellar polarization, and the nebular axes might be better aligned with the local interstellar polarization than with the galactic plane. This is particularly interesting to investigate for those misaligned objects.

The position angle of each nebula is therefore compared to the polarization position angles of the nearest neighbouring stars on the celestial sphere. The polarization data are taken from the Axon & Ellis (1976) compilation, the data related to the nebula central stars themselves being discarded. Since the considered LBV and WR nebulae are rather distant objects (Table 1), only distant stars ($d_{star} \geq 400$ pc) are accounted for, i.e. those stars lying beyond the local volume where most interstellar polarization is imprinted. Also, only sufficiently polarized objects are considered i.e. those with a polarization degree $p \geq 0.2\%$. Then if $\theta_{\rm ISM}$ refers to the interstellar polarization position angle of a given star, we evaluate the angle difference

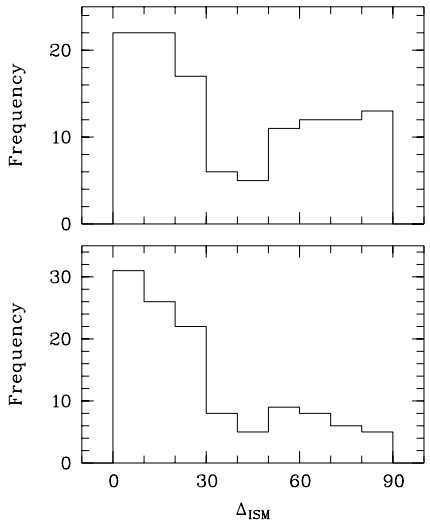

Fig. 3. *Top:* the distribution of $\Delta_{\rm ISM}$, the difference between the position angle of the nebulae and the interstellar polarization position angle of neighbouring stars. For each nebula the ten nearest stars are considered. *Bottom:* the distribution of $\Delta_{\rm ISM}$ after rotating by 90° the major axes of the three nebulae which are nearly perpendicular to the galactic plane

$$\Delta_{\rm ISM} = 90^\circ - |90^\circ - |\theta_{\rm G} - \theta_{\rm ISM}|| \qquad (2)$$

for each nebula and its ten polarized nearest neighbours. In general, the ten neighbouring stars are within a few degrees from the objects.

Fig. 3 illustrates the distribution of $\Delta_{\rm ISM}$. It appears bimodal and indicates an overall alignment, as expected from the distribution of the nebular position angles. Also illustrated is the distribution of $\Delta_{\rm ISM}$ computed after rotating by 90° the axes of the three nebulae which are nearly perpendicular to the galactic plane. In this case the peak near $\Delta_{\rm ISM}$ = 0° is definitely stronger. This indicates that misaligned objects are not better aligned with the interstellar polarization than with the galactic plane. This is also illustrated in Fig. 4 where nebulae with various orientations are represented. Only the nebula around WRA751, the axis of which is not parallel nor perpendicular to the galactic plane, is possibly better aligned with the neighbouring interstellar polarization vectors. However, it should be clear that we cannot conclude from these results that the nebulae which are perpendicular to the interstellar polarization vectors are necessarily perpendicular to the direction of the interstellar magnetic field in their direct vicinity. Indeed, the interstellar polarization from the compilation of Axon & Ellis (1976) is measured from stars which are generally closer to us or closer to the galactic plane than the considered nebulae.

3.3. Alignment of nebulae with the magnetic field in the LMC

A completely different, external, point of view is provided from the LMC which is seen at medium inclination. In this case, the nebular axes may be directly compared to the magnetic field lines.

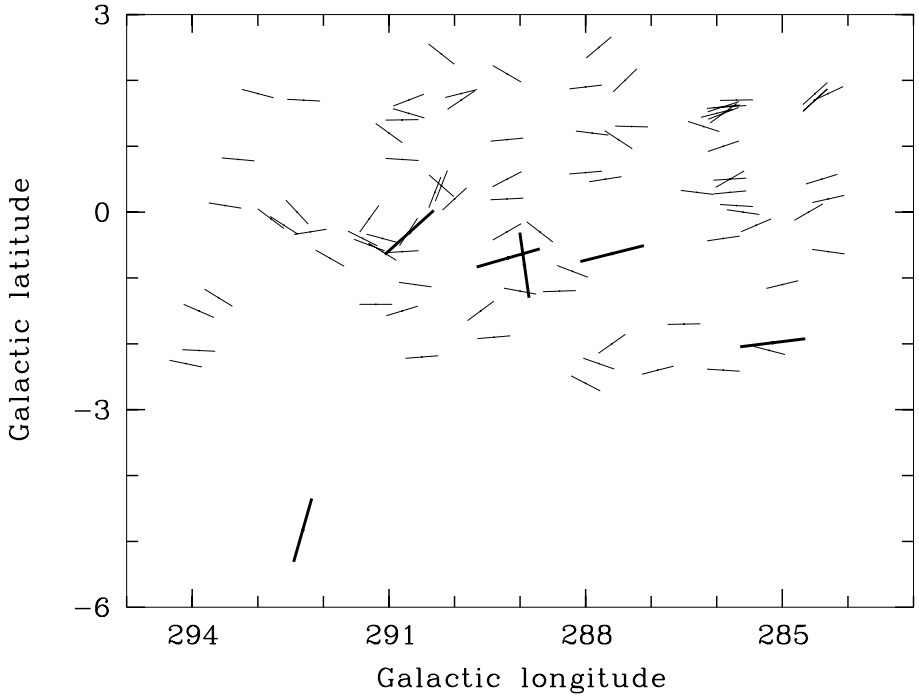

Fig. 4. A map of the interstellar polarization in the Carina region where several LBV and WR nebulae are located. All polarized stars with $d_{star} \geq 400\,\mathrm{pc}$ and $p \geq 0.2\%$ from the Axon & Ellis (1976) catalogue are represented. The vector length is arbitrary. The six superimposed thick lines represent the nebular long axes of HR Car, AG Car, η Car (roughly aligned with the galactic plane), He3-519, RCW58 (roughly perpendicular to the galactic plane), and WRA751

Using radio polarization measurements, Klein et al. (1993) have obtained a well-sampled map of the LMC magnetic field (which they found in overall good agreement with the optical polarization). The data were kindly provided by the authors, and are illustrated in Fig. 5 together with the long axes of the four considered nebulae (Table 2). We can see that the nebular axes closely follow the LMC magnetic field. We then evaluate the mean direction of the LMC magnetic field in the vicinity of each nebula, $\bar{\theta}_{\rm B}$, by vectorially averaging the five nearest data points (i.e. roughly within half a degree around the objects). The difference $\Delta_{\rm B}$ is then computed using

$$\Delta_{\rm B} = 90^\circ - |90^\circ - |\theta_{\rm E} - \bar{\theta}_{\rm B}||\,, \qquad (3)$$

and given in Table 2. All the $\Delta_{\rm B}$ values are small, clearly indicating that LBV-type nebulae, as well as the nebula around SN1987A, are aligned with the LMC magnetic field.

The sample of LBV-type nebulae from the LMC is unfortunately too small to derive a useful statistical significance for the observed alignment. However, in light of our previous results obtained for galactic nebulae (Sect. 3.1), this alignment with the LMC magnetic field clearly provides additional evidence for a correlation between LBV-type nebula orientations and galactic magnetic fields.

Note that from our results in the Galaxy, we would also expect the nebular axes to be aligned with the plane of the LMC. This may be verified for the SN1987A nebula since its inclination with respect to the line of sight has been estimated: $i \simeq 45^\circ$ (Burrows et al. 1995, Meaburn et al. 1995). Assuming the LMC inclined at $\sim 45^\circ$ with a line of nodes at a position angle $\simeq 190^\circ \pm 20^\circ$ (Westerlund 1990), we find that the long axis of the SN1987A nebula is tilted by $\sim 18^\circ \pm 10^\circ$ from the LMC plane. In this case, the east side of the LMC being closer to us implies that the southern part of the SN1987A nebula is nearer us, as observed (Burrows et al. 1995). This result indicates that the long axis of the SN1987A nebula is reasonably aligned with the LMC plane, though the uncertainties of the involved quantities are large.

4. Conclusions and discussion

In the present study we find evidence for a correlation between the orientation of the long axes of nebulae ejected by massive stars and the global structure of the galaxy to which they belong. The Galaxy and the LMC offer complementary views of the same phenomenon. In the Galaxy, the axes are essentially found aligned with the galactic plane, and then also with the galactic magnetic field. The effect is statistically significant. In the LMC, the axes closely follow the magnetic field lines, supporting the correlation between nebular orientations and galactic structure. The latter result suggests a major role of the magnetic field in the alignment effect as opposed to a purely dynamical mechanism, although the magnetic structure in the LMC is probably intimately related to the dynamical structure as in large spiral galaxies (Klein et al. 1993).

The present sample of LBV-type nebulae is unfortunately small, and a confirmation of the effect will await new discoveries of similar objects, especially in external galaxies. Misaligned nebulae could be important for unambiguously identifying the dominant role of the magnetic field. If it ultimately appears that the misalignment with the galactic plane is real and not due to errors in the interpretation of morphological features, these nebulae could align with more local structures in the interstellar magnetic field, like the large-scale magnetic field loops which extend at high galactic latitudes (e.g. Mathewson & Ford 1970). More detailed studies of these objects are therefore needed to

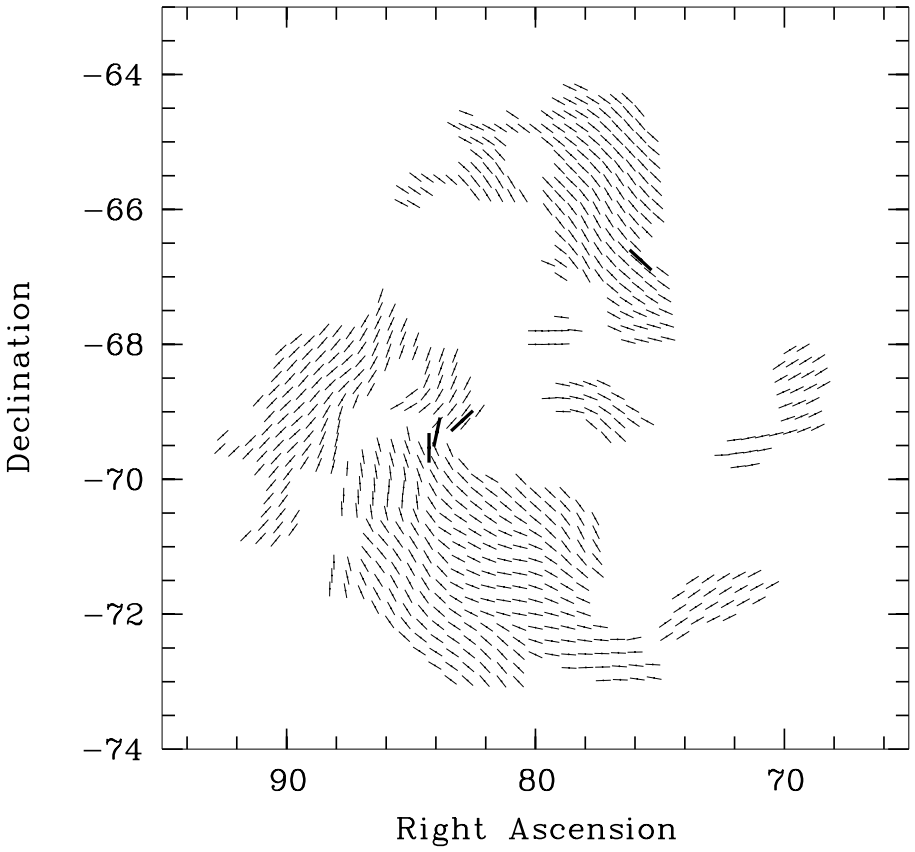

Fig. 5. A map of the LMC magnetic field from the radio polarization measurements of Klein et al. (1993). The long axes of the nebulae associated with R127, S119, Br13 and SN1987A are superimposed

determine their true morphology[4], as well as the direction of the interstellar magnetic field in their environs.

At the origin of the observed alignment, one could invoke the direct effect of the ambient interstellar magnetic field on the nebular morphology. But, as discussed by several authors in the context of planetary nebulae (Heiligman 1980, Phillips 1997), if the ambient magnetic field can induce small modifications to the morphology, it is not able to shape the outflowing material. This is a fortiori true for the more massive nebulae around LBV and WR stars. More likely, the nebular axis is correlated to the symmetry (rotation) axis of the star and/or to the orientation of a preexisting disk (which could be magnetized). These symmetry axes are themselves related to the direction of the ambient magnetic field from the star formation process. Such a scenario, already suggested by Aitken et al. (1995) for η Car, is supported by several arguments. Indeed, Schulte-Ladbeck et al. (1993, 1994) and Clampin et al. (1995) have shown from polarization studies that the morphological axes of the nebulae surrounding the LBVs R127, AG Car and HR Car are related to the symmetry axes of the stellar winds, and consequently most probably to those of the stars. From the theoretical point of view, a relic protostellar disk or an equatorially compressed outflow due to stellar rotation, both with relative importance which may differ from one object to another, are welcome to explain the preexisting density contrast needed to explain the shapes of LBV nebulae (Nota et al. 1995). Such a density contrast is expected to be perpendicular to the nebular long axis. Finally, disks around young stars are known to be perpendicular to the interstellar magnetic field, the outflows themselves being parallel. This is apparently a key feature of the star formation process which is reproduced by a variety of models (e.g. Pudritz & Norman 1986, Strom et al. 1988, Appenzeller 1989). In this context, it is remarkable that the large-scale distribution of molecular gas around η Car (as shown in Cox 1995) appears to have roughly the same orientation as the homunculus.

Whatever the mechanism which causes it, it is quite striking that an alignment with the galactic plane or with the galactic magnetic field has been reported for several types of objects, from planetary nebulae[5] to supernova remnants (e.g. Gaensler 1998, and references therein), although it is not clear whether all nebula sub-classes do show an alignment effect, and if it also prevails out of the galactic plane (cf. Grinin & Zvereva 1968, Gaensler 1998). The alignment with galactic structures, and more particularly with galactic magnetic fields, could there-

[4] As far as the alignment effect is considered, the knowledge of the 3D orientation does not bring much additional information for nebulae which are already aligned in projection with the galactic plane. However, it is important for those misaligned nebulae (which may be seen nearly pole-on; cf. also Sect. 2), as well as for nebulae seen in external galaxies inclined as the LMC

[5] While most authors have found an alignment of planetary nebulae major axes with the galactic plane (cf. Sect. 1), Corradi et al. (1998) have just published a new study which seriously questions the reality of the effect

fore be a generic property of nebulae ejected by evolved stars. Note this does not mean that the same mechanism is at work in all cases. For example, the morphology of supernovae remnants may follow the cavity created by previous ejecta (and namely the LBV/WR stellar winds and nebulae) as suggested by Bisnovatyi-Kogan et al. (1990). In this view, it is interesting to note that the radio remnant of SN1987A seems to follow the morphology of the optical nebula (Gaensler at al. 1997). Also, mechanisms of star formation may substantially differ for massive and low-mass stars (e.g. Shepherd & Churchwell 1996), and more particularly the relative influence of the interstellar magnetic field in the early stages of formation (Mestel & Subramanian 1991).

As a whole, the dynamical effect of such collective non-isotropic gas and dust ejections along preferred directions – and especially from the most massive stars– could be important for a detailed understanding of the interstellar medium evolution, including in starbursts. And one may further speculate that it might provide a natural explanation to some viewing angle effects discussed in the context of stellar ejecta models proposed for active galactic nuclei and broad absorption line quasars.

Acknowledgements. I am particularly grateful to Professor Ulrich Klein for providing me with his data on the LMC magnetic field. I also thank H. Lamy for independently measuring some dubious nebular axes, and E. Gosset, G. Rauw and the referee for useful comments on the manuscript. The catalogue of Axon & Ellis has been retrieved in electronic form thanks to the Centre de Données Stellaires (CDS) in Strasbourg, France.

Appendix A: position angle (P.A.) measurements: notes on individual objects

HD168625: The emission nebula surrounding HD168625 consists of an elliptical ring from which seems to emerge a bipolar nebula (Hutsemékers et al. 1994, Nota et al. 1996). After several measurements from these published images, we estimate the long bipolar axis to be oriented at P.A. = 29°± 5°.

G25.5+0.2: On the radio and near-infrared images displayed by Subrahmanyan et al. (1993), the very distant nebula G25.5+0.2 appears roughly bipolar, with two brighter condensations along the minor axis. From these images, we estimate P.A. = 128°± 5° for the long nebular axis.

M1-67: The nebula M1-67 is associated with the WN8 star 209 BAC (WR124). On the images in Chu & Treffers (1981) and Solf & Carsenty (1982) it appears as a clumpy nebula without definite bipolar or elliptical morphology. It is nevertheless elongated along one direction, and Solf & Carsenty (1982) give P.A. ≃20° for its long axis. On the basis on these published images plus new ones obtained with EFOSC, we adopt P.A. = 25°± 10°.

NGC6888: The nebula NGC6888 surrounding the WN6 star HD 192163 (WR136) is nicely illustrated in Miller & Chu (1993). The overall morphology looks roughly elliptical, or bipolar with a possible "waist". Marston & Meaburn (1988) give P.A. = 35° for the long axis orientation. After additional measurements from the Miller & Chu (1993) Hα+[N II] image, we adopt P.A. = 38°± 3°.

G79.29+0.46: The nebula G79.29+0.46 has been imaged at radio wavelengths by Higgs et al. (1994). The nebula appears as a nearly circular ring, slightly elongated in the north-east direction. A faint spur is also seen in this direction, external to the ring. We adopt P.A. = 45°± 10° for the major axis of the ellipse.

S308: The nebula S308 surrounds the WN5 star HD50896 (WR6). On the [O III] images shown by Chu et al. (1982), the nebula appears nearly circular with a funnel-shaped elongation. Although this morphology is less typical (as compared to younger LBV nebulae), it is nevertheless reminiscent of a bipolar lobe (rather small here) with brighter condensations along the perpendicular axis. We therefore assume the long axis going through this elongation and we adopt P.A. = 146°± 10°. Note that a distant funnel-shaped nebulosity aligned with the nebula long axis has been found in the vicinity of HR Car (Weis et al. 1997).

HR Car: The HR Car nebula was recently identified as a true bipolar nebula by Weis et al. (1997) and Nota et al. (1997). These authors respectively give P.A. = 125° and 135° for the nebula long bipolar axis. We adopt P.A. = 130°± 5°. The comparison with the discovery images in Hutsemékers & Van Drom (1991a) illustrates the importance of good quality data for measuring accurate position angles.

η Car: The famous homunculus surrounding η Car is mainly a reflection nebula whose morphology is clearly bipolar. The orientation of its long axis is well defined and Meaburn et al. (1993) give P.A. = 132°. We adopt P.A. = 132°± 2°.

He3-519: The nebula around He3-519 appears as an elliptical ring, roughly box-shaped (Stahl, 1987). The P.A. of the major axis is measured from the image shown in Stahl (1987), plus additional ones we obtained with EFOSC. We find P.A. = 34°± 5°.

AG Car: The emission nebula around AG Car is ring-like, roughly elliptical. Smith (1991) and Schulte-Ladbeck et al. (1994) respectively give P.A. = 131° and 135° for the major axis. After additional measurements namely from our EFOSC images, we adopt a mean P.A. of 132°± 3°.

WRA751: On the images shown in Hutsemékers & Van Drom (1991b), the nebula around WRA751 appears nearly circular, slightly extended along P.A. ∼ 160°. Additional images obtained with EFOSC reveal a more complex ring-like morphology with arcs and ansae. The orientation of the long axis lies between P.A. = 145° and 165°. We adopt P.A. = 155°± 10°.

RCW58: The nebula RCW58 surrounds the WN8 star HD96548 (WR40). In Hα it appears as an elliptical ring (Chu 1982, Smith et al. 1988, Marston 1996). When measured from these published images, we estimate the major axis to be oriented at P.A. = 8°±5°.

Br13: The nebula around the WN8 star Br13 in the LMC appears elliptical on the Hα images displayed by Garnett & Chu (1994). From these images, we measure P.A. = 47°±3° for the major axis.

S119: Nota et al. (1995) found the nebula surrounding the LMC Of/WN star S119 apparently elliptical with a very bright con-

densation along the minor axis. From their published [N II] image, we estimate the major axis to be oriented at P.A. = 133°±5°.

SN1987A: Although its true nature is far from clear, the three-ring nebula associated with SN1987A in the LMC has an overall bipolar morphology (Burrows et al. 1995). Using Hubble Space Telescope images available in the literature (Burrows et al. 1995, Panagia et al. 1996), we measure P.A. = 168°±5° for the long axis of the whole nebula.

R127: Images of the nebula surrounding the LBV R127 in the LMC are shown in Clampin et al. (1993) and Nota et al. (1995). The nebula is essentially elliptical. Clampin et al. (1993) found the major axis lying at P.A. = 165°. Since the definition of the axis may be affected by the subtraction of neighbouring stars (cf. Clampin et al. 1993), we also take into account the P.A. of the minor axis, assuming it is perpendicular to the major one. Schulte-Ladbeck et al. (1993) have estimated the P.A. of the minor axis between 90° and 100°. After some additional measurements, we adopt P.A. = 180°±10° for the orientation of the nebula major axis.

References

Aitken D.K., Smith C.H., Moore T.J.T., Roche P.F., 1995, MNRAS 273, 359

Appenzeller I., 1989, In: Delache P., et al. (eds.) Modeling the Stellar Environment. 4th IAP Astrophysics Meeting, p. 47

Axon D.J., Ellis R.S., 1976, MNRAS 177, 499

Bisnovatyi-Kogan G.S., Lozinskaya T.A., Silich S.A., 1990, ApSS 166, 277

Burrows C.J., Krist J., Hester J.J., et al., 1995, ApJ 452, 680

Chu Y.-H., Treffers R.R, 1981, ApJ 249, 586

Chu Y.-H., 1982, ApJ 254, 578

Chu Y.-H., Gull T.R., Treffers R.R., Kwitter K.B., Troland T.H., 1982, ApJ 254, 562

Clampin M., Nota A., Golimowski D.A., Leitherer C., Durrance S.T., 1993, ApJ 410, L35

Clampin M., Schulte-Ladbeck R.E., Nota A., et al., 1995, AJ 110, 251

Corradi R.L.M., Aznar R., Mampaso A., 1998, MNRAS 297, 617

Cox P., 1995, Rev. Mex. Astron. Astrofis. 2, 105

Fisher N.I., 1993, Statistical Analysis of Circular Data. Cambridge University Press, Cambridge

Fisher N.I., Lewis T., Embleton B.J.J., 1987, Statistical Analysis of Spherical Data. Cambridge University Press, Cambridge

Gaensler B.M., Manchester R.N., Staveley-Smith L., et al., 1997, ApJ 479, 845

Gaensler B.M., 1998, ApJ 493, 781

Garnett D.R., Chu Y.-H., 1994, PASP 106, 626

Grinin V.P., Zvereva A.M., 1968, In: Osterbrock D.E., O'Dell C.R. (eds.) Planetary Nebulae. IAU Symp. 34, p. 287

Heiligman G.M., 1980, MNRAS 191, 761

Higgs L.A., Wendker H.J., Landecker T.L., 1994, A&A 291, 295

Hutsemékers D., Van Drom E., 1991a, A&A 248, 141

Hutsemékers D., Van Drom E., 1991b, A&A 251, 620

Hutsemékers D., 1994, A&A 281, L81

Hutsemékers D., Van Drom E., Gosset E., Melnick J., 1994, A&A 290, 906

Hutsemékers D., 1997, In: Nota A., Lamers H. (eds.) Luminous Blue Variables: Massive Stars in Transition. ASP Conf. Ser. 120, p. 316

Klein U., Haynes R.F., Wielebinsky R., Meinert D., 1993, A&A 271, 402

Marston A.P., 1996, In: Vreux J.-M., et al. (eds.) Wolf-Rayet Stars in the Framework of Stellar Evolution. 33rd Liège Int. Astrophys. Coll., p. 445

Marston A.P., Meaburn J., 1988, MNRAS 235, 391

Mathewson D.S., Ford V.L., 1970, Mem. R. Ast. Soc. 74, 139

Meaburn J., Walsh J.R., Wolstencroft R.D., 1993, A&A 268, 283

Meaburn J., Bryce M., Holloway A.J., 1995, A&A 299, L1

Melnick G., Harwit M., 1975, MNRAS 171, 441

Mestel L., Subramanian K., 1991, MNRAS 248, 677

Miller G.J., Chu Y.-H., 1993, ApJS 85, 137

Nota A., Livio M., Clampin M., Schulte-Ladbeck R., 1995, ApJ 448, 788

Nota A., Pasquali A., Clampin M., et al., 1996, ApJ 473, 946

Nota A., Clampin M. 1997, In: Nota A., Lamers H. (eds.) Luminous Blue Variables: Massive Stars in Transition. ASP Conf. Ser. 120, p. 303

Nota A., Smith L.J., Pasquali A., Clampin M., Stroud M., 1997, ApJ 486, 338

Panagia N., Scuderi S., Gilmozzi R., et al., 1996, ApJ 459, L17

Phillips J.P., 1997, A&A 325, 755

Pudritz R.E., Norman C.A., 1986, ApJ 301, 571

Schulte-Ladbeck R.E., Leitherer C., Clayton G.C., et al., 1993, ApJ 407, 723

Schulte-Ladbeck R.E., Clayton G.C., Hillier D.J., Harries T.J., Howarth I.D., 1994, ApJ 429, 846

Shepherd D.S., Churchwell E., 1996, ApJ 472, 225

Smith L.J., Pettini M., Dyson J.E., Hartquist T.W., 1988, MNRAS 234, 625

Smith L.J. 1991, In: van der Hucht K.A., Hidayat B. (eds.) Wolf-Rayet Stars and Interrelations with Other Massive Stars in Galaxies. IAU Symp. 143, p. 385

Smith L.J., 1995, In: van der Hucht K.A., Williams P.M. (eds.) Wolf-Rayet Stars: Binaries, Colliding Winds, Evolution. IAU Symp. 163, p. 24

Solf J., Carsenty U., 1982, A&A 116, 54

Stahl O., 1987, A&A 182, 229

Strom S.E., Strom K.M., Edwards S., 1988, In: Pudritz R.E., Fich M. (eds.) Galactic and extragalactic star formation. Kluwer Academic, p. 53

Subrahmanyan R., Ekers R.D., Wilson W.E., Goss W.M., Allen D.A., 1993, MNRAS 263, 868

Weis K., Duschl W.J., Bomans D.J., Chu Y.-H., Joner M.D., 1997, A&A 320, 568

Westerlund B.E., 1990, A&AR 2, 29